Two-dimensional steady-state photorefractive screening solitons

Ming-feng Shih, Patrick Leach, and Mordechai Segev

Department of Electrical Engineering and Advanced Center for Photonics and Optoelectronic Materials, Princeton University, Princeton, New Jersey 08544

Mark H. Garrett

Deltronic Crystal Industries, Dover, New Jersey 07801

Greg Salamo

Department of Physics, University of Arkansas, Fayetteville, Arkansas 72701

George C. Valley

Hughes Research Laboratories, Malibu, California 90265

Received September 13, 1995

We study experimentally steady-state photorefractive screening solitons trapped in both transverse dimensions and measure their beam profiles as they propagate throughout the crystal. The solitons are observed to be axially symmetric, and they self-bend. We characterize the soliton dependence on the optical intensity, applied electric-field strength, and beam diameter. © 1996 Optical Society of America

Spatial solitons in photorefractive media[1] have attracted much interest in the past few years. At present, three types of scalar soliton have been found. First, a suitable external field applied to a photorefractive crystal supports transient bright and dark solitons, trapped in one and two transverse dimensions (named *quasi-steady-state solitons*).[1,2] Second, photorefractive–photovoltaic materials support bright and dark steady-state *photovoltaic solitons*.[3] Third, application of an external electric field also permits steady-state photorefractive solitons, as suggested by Iturbe-Castillo *et al.*[4] based on one-dimensional (1-D) steady-state self-focusing observations in $Bi_{12}TiO_{20}$. The theory of steady-state solitons was formulated in Refs. 5 and 6, and these were named *screening solitons*.[5] They result from spatially nonuniform screening of the applied field, which lowers the refractive index away from the center of the optical beam and forms a waveguide. Recently, screening solitons trapped in both transverse dimensions were reported.[7] Here we study the two-dimensional (2-D) steady-state screening soliton, report detailed measurements of soliton properties, and show that the solitons can be axially symmetric.

In one transverse dimension, our calculations show that the narrowest screening soliton is obtained for soliton peak intensities roughly three times larger than the sum of the background and the dark irradiances.[5] We use background intensities of mW/cm^2 (much greater than the dark irradiance), which permit observations of 1–10-μW solitons with 0.1–1-s response times in strontium barium niobate (SBN).[7] The background irradiance is provided by a laser beam illuminating the crystal uniformly and polarized orthogonally to the soliton beam. Since our 1-D calculations showed that the soliton depends on the intensity ratio (rather than on absolute intensity, as in Kerr media), it is important to keep that ratio constant throughout propagation even in the presence of absorption. We therefore launch copropagating soliton and background beams.

We generate the screening solitons in SBN:60 by launching an extraordinarily polarized TEM_{00} beam ($\lambda = 514$ nm) along the crystalline a axis.[7] A typical top-view photograph of a 10-μm-diameter (FWHM) soliton propagating for 5.5 mm is shown in Fig. 1 (upper trace). An axially symmetric soliton with an intensity ratio of 70 required 3400 V applied along the crystalline c axis between electrodes separated by 5.5 mm. Within the resolution of our top-view imaging system (± 4 μm), the soliton beam did not experience any changes in its diameter. A slightly lower voltage generated an elliptical soliton beam that is narrower in the direction parallel to the external field, whereas a slightly higher voltage gives rise to a soliton narrower in the direction perpendicular to the field. At zero voltage the beam diffracts to roughly 57-μm FWHM diameter,[8] as shown by the lower trace in Fig. 1. Using interferometry, we determine that the transverse phase of the soliton at the exit face of the crystal is uniform. Hence, the soliton beam at the exit face acts as a minimal waist, and Gaussian-beam optics can be used to image it onto a CCD camera.[7] The soliton is stable and reshapes itself; hence one does not have to launch a beam of the proper (soliton) size, but rather the soliton evolves into its stationary shape and size. Figure 2 compares the evolution of input beams of different sizes and transverse phase under fixed voltage and intensity ratio. Figure 2(a) shows 12-μm (FWHM) input beam profiles (upper traces), the diffracted output profiles at zero voltage (middle traces), and the 12-μm soliton

0146-9592/96/050324-03$6.00/0

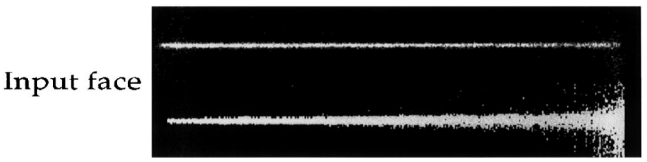

Fig. 1. Top-view photograph of a 10-μm soliton (upper trace) and a normally diffracting beam (lower trace) propagating along a 5.5-mm crystal.

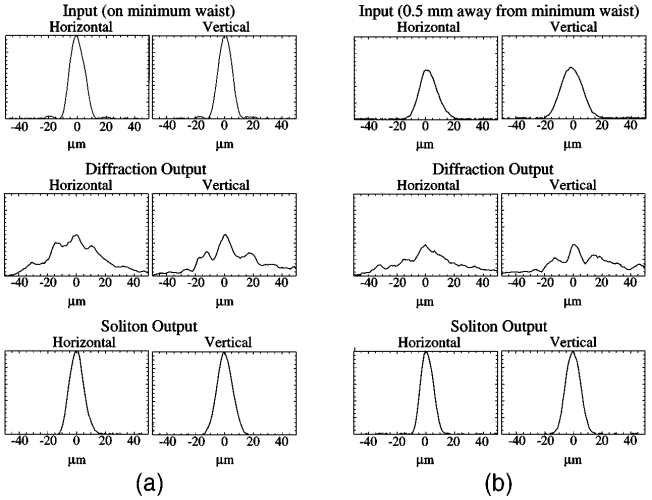

Fig. 2. Horizontal and vertical profiles of the input (upper traces), diffracted output (middle traces), and soliton output (lower traces) beams when the input face of the crystal is (a) at the minimum waist of the input beam and (b) 500 μm away from the minimum waist.

output profiles (lower traces) when the input face of the crystal is located at its minimal waist of the input beam. Figure 2(b) shows 17-μm input beam profiles (upper traces), the diffracted output profiles at zero voltage (middle traces), and the 12-μm soliton output profiles (lower traces) when the input face of the crystal is located 500 μm away from the minimal waist. Although the beams differ by 40% in width and significantly in their transverse phases, the output soliton profiles are nearly identical. The soliton stability and reshaping are also seen by comparing the profiles of the diffracted beams (Fig. 2, middle traces), significantly perturbed by material inhomogeneities, with the smooth soliton profiles (Fig. 2, lower traces).

To investigate soliton evolution, it is desirable to image the soliton beam profile as it propagates throughout the crystal. For this purpose we cut a SBN crystal at 15° with the a axis (Fig. 3) and launch the soliton at different propagation distances by translating the beam laterally (keeping all other parameters unchanged). By imaging the beam profile at the crystal output face, we obtain the soliton profiles for propagation distances of 3.15 to 3.85 mm shown in Fig. 3 (keeping a safe distance from the edges of the crystal). Within the 1-μm resolution of our front imaging system, the soliton beam maintains a constant 12-μm profile throughout the entire propagation distance. At zero voltage the beam diffracts from 12 μm at the input face to 26 μm at the shortest propagation distance (3.15 mm) and to 34 μm at the largest distance (3.85 mm).

To investigate axial symmetry of the soliton in our specially cut crystal, consider a soliton incident upon a dielectric interface (crystal–air) slanted at 15° (Fig. 3, lower right). The beam is deflected by the interface to 37.5° with the normal to the surface (refractive index ≈2.35). The beam profile normal to the plane of the drawing (the profile parallel to the c axis) is transformed as is to air without a change in size, while the profile in the plane is altered by the deflection, together producing a 2-D beam that looks elliptical. Since the soliton beam has a uniform transverse phase, its diameter d is transformed into a (slanted) diameter $d' = d\cos(37.5°)/\cos(15°) \approx 0.82d$, which is what we image experimentally. For an axially symmetric 12-μm-wide soliton beam, we obtain the imaged profiles shown at the left in Fig. 3, which are elliptical with $d' = 10$ μm and $d = 12$ μm. Thus we conclude

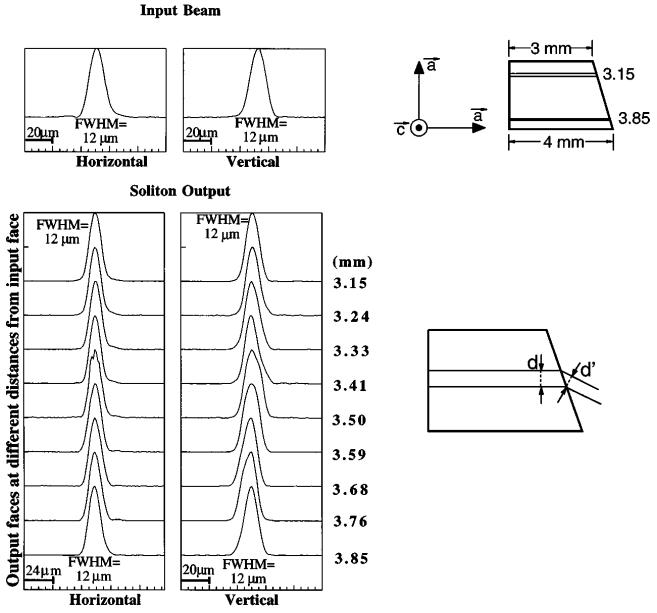

Fig. 3. Left: Beam profiles at the crystal input face (upper traces) and soliton beam profiles, normalized to their peak intensities, at various output planes of the specially cut SBN crystal (lower traces). The values give the actual sizes of the profiles, but their shapes are as imaged (with the astigmatism introduced by Snell's law). Upper right: The specially cut crystal and its crystalline orientation; lower right: Snell's law in this configuration.

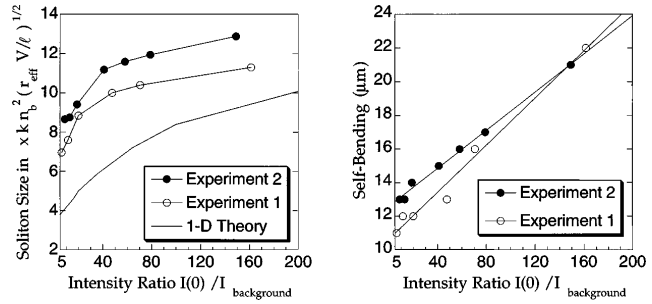

Fig. 4. Left: Widths of a 2-D axially symmetric soliton measured in two different SBN crystals and the calculated width of a 1-D soliton as a function of the ratio between the soliton peak intensity and the background irradiance. Right: Self-bending offset as a function of intensity ratio for solitons in these crystals.

that the soliton maintains a constant profile and diameter during propagation and is axially symmetric.

Although our theory[5] analyzes 1-D solitons, we can compare it with experiments with 2-D solitons. The theory[5] shows that a 1-D soliton of a given diameter and intensity ratio exists at a single value of external field. To investigate this qualitatively for 2-D solitons, we perform a series of experiments with axially symmetric solitons of various diameters in normal-cut crystals. *We find that for a 2-D soliton for each value of intensity ratio there exists a single value of applied field that supports an axially symmetric soliton.* Figure 4 shows the soliton width (FWHM) in normalized units ξ as a function of the intensity ratio, where $\xi = xkn_b^2\sqrt{r_{33}V/\ell}$, with x the soliton diameter in dimensional units, k the wave number in vacuum, n_b the background refractive index, and V the voltage applied between electrodes separated by ℓ. The trend is similar to that predicted by the 1-D theory. The range of intensity ratio is limited by surface breakdown currents (at large ratios, which require higher fields) and by instability (the beam varies continuously in time, never reaching steady state) of the soliton beam at low ratios. The instability at low ratios may be associated with striations, which spatially modulate the background irradiance, or, since in this limit the nonlinearity resembles the Kerr nonlinearity,[5] the instability may be fundamental, because 2-D Kerr solitons are inherently unstable. For intensity ratios >5, the 2-D soliton is stable.

Singh and Christodoulides[6] predicted that solitons should self-bend[9] toward the c axis and maintain their shape. This results from the diffusion field, which is the first correction to the leading term $1/(1 + I)$ in the space-charge field (which traps the soliton).[5] The magnitude of self-bending is a function of the intensity ratio, the diffusion, and the applied fields. We measure self-bending as large as 20 μm, by measuring the distance from the center of the diffracted beam to the center of the soliton immediately after turning the beam on (before the diffusion field evolves). Figure 4 shows the measured self-bending offset in micrometers as a function of intensity ratio which appears to obey a linear relation.

Finally, we note that Zozulya and Anderson[10] state that the evolution of a Gaussian-type beam in a biased photorefractive crystal is characterized by oscillations of its diameters in both transverse axes and by spreading, uncharacteristic of solitons. Their numerics predict oscillations from 35 to 17.5 μm every 2 mm. Figures 1–3 here and Ref. 7 suggest that these simulations are in a very different regime from the solitons that we observe. The observed soliton beam maintains a constant diameter (Figs. 1 and 3), and no oscillations in its diameter are observed. A possible reason for the disagreement with Ref. 10 is that solitons exist for a specific set of parameters, as shown by our 1-D calculations[5] and in Fig. 4. In a given crystal a soliton of a specific diameter at a given value of intensity ratio exists at a single value of the external field. Furthermore, even in the 1-D case "optical beams that significantly differ from soliton solutions tend to experience cycles of compression and expansion."[6] Apparently, the parameters used in that numeric[10] were too far from those that can support a soliton. Even a Gaussian beam propagating in Kerr media[11] is characterized by oscillations in its diameter, and the beam coverges to a soliton only if the parameters are close enough to the soliton parameters. We observe that when we detune the applied field or the intensity ratio by more than 20% from the soliton values the beam breaks up (fields too high for that intensity ratio) or does not form (field too low; only self-focusing observed). We conclude that the numerical work of Ref. 10 does not describe the experimental results presented here. Note that our observations of axially symmetric solitons do not contradict calculations[10,12] that predict a strong astigmatism of the induced lens in the regime in which the intensity ratio is much less than 1, since the 2-D solitons could never be observed in this regime.

The authors thank A. E. Kaplan of Johns Hopkins University for the idea of imaging the soliton using a specially cut crystal. M. Segev gratefully acknowledges the generous support of the Sloan Fellowship and of Hughes Research Laboratories.

References

1. M. Segev, B. Crosignani, A. Yariv, and B. Fischer, Phys. Rev. Lett. **68,** 923 (1992).
2. G. Duree, J. L. Shultz, G. Salamo, M. Segev, A. Yariv, B. Crosignani, P. DiPorto, E. Sharp, and R. R. Neurgaonkar, Phys. Rev. Lett. **71,** 533 (1993); **74,** 1978 (1995).
3. G. C. Valley, M. Segev, B. Crosignani, A. Yariv, M. M. Fejer, and M. Bashaw, Phys. Rev. A **50,** R4457 (1994); M. Taya, M. Bashaw, M. M. Fejer, M. Segev, and G. C. Valley, Phys. Rev. A **52,** 3095 (1995).
4. M. D. Iturbe-Castillo, P. A. Marquez-Aguilar, J. J. Sanchez-Mondragon, S. Stepanov, and V. Vysloukh, Appl. Phys. Lett. **64,** 408 (1994).
5. M. Segev, G. C. Valley, B. Crosignani, P. DiPorto, and A. Yariv, Phys. Rev. Lett. **73,** 3211 (1994); M. Segev, M. Shih, and G. C. Valley, "Photorefractive screening solitons of high and low intensity," J. Opt. Soc. Am. B (to be published).
6. S. R. Singh and D. N. Christodoulides, Opt. Commun. **118,** 569 (1995).
7. M. Shih, M. Segev, G. C. Valley, G. Salamo, B. Crosignani, and P. DePorto, Electron. Lett. **31,** 826 (1995).
8. The Gaussian beam here diffracts from 10 to 57 μm FWHM after 5.5 mm in a crystal, which corresponds to diffraction from 16.7 to 94 μm at the $1/e$ points. The diffracted value in Ref. 6 ($\approx$100 μm) is 60 μm FWHM.
9. Self-bending was first predicted for Kerr media by A. E. Kaplan, JETP Lett. **9,** 59 (1969).
10. A. A. Zozulya and D. Z. Anderson, Opt. Lett. **20,** 837 (1995); Phys. Rev. A **51,** 1520 (1995); in *Digest of Photorefractive Materials, Effects, and Devices Topical Meeting* (Optical Society of America, Washington, D.C., 1995), paper TC4.
11. D. Burak and W. Nasalski, Appl. Opt. **33,** 6393 (1994).
12. C. M. Gomez, P. A. Marquez-Aguilar, J. J. Sanchez-Mondragon, S. Stepanov, and V. Vysloukh, in *Digest of Photorefractive Materials, Effects, and Devices Topical Meeting* (Optical Society of America, Washington, D.C., 1995), paper TC2.